The Hydrophobic Effect and the Influence of Solute−Solvent Attractions

David M. Huang and David Chandler*

Department of Chemistry, University of California at Berkeley, Berkeley, California 94720

Received: August 25, 2001; In Final Form: November 29, 2001

We have studied the effect of weak solute−solvent attractions on the solvation of nonpolar molecules in water at ambient conditions using an extension and improved parameterization of the theory of solvation due to Lum, Chandler, and Weeks [*J. Phys. Chem. B* **1999**, *103*, 4570]. With a reasonable strength of alkane−water interactions, an accurate prediction of the alkane−water interfacial tension is obtained. As previously established for solutes with no attractive interactions with water, the free energy of solvation scales with volume for small solutes and with surface area for large solutes. The crossover to the latter regime occurs on a molecular length scale. It is associated with the formation of a liquid−vaporlike interface, a drying interface, between the large hydrophobic solute and liquid water. In the absence of attractions, this interface typically lies more than one solvent molecular diameter away from the hard sphere surface. With the addition of attractive interactions between water and the hard sphere, the average separation of the interface and solute surface is decreased. For attractive force strengths typical of alkane−water interactions, we show that the drying interface adjacent to a large hydrophobic solute remains largely intact, but is moved into contact with the solute surface. This effect results from the "soft modes" characterizing fluctuations of liquid−vapor interfaces. We show that attractive interactions are of almost no consequence to the temperature dependence of the solvation free energies relevant to protein folding.

I. Introduction

Theory and simulation for hard spheres or bubbles in water have established an important crossover between small and large length scale hydrophobicity.[1−5] At small length scales, where the spheres have radii significantly less than 1 nm, the solvation free energy scales linearly with the volume excluded by the solute. At large length scales, where the spheres (or spherical collection of spheres) have radii larger than 1 nm, the solvation free energy scales linearly with the surface area of that excluded volume. The crossover to the large length scale regime is associated with the formation of a liquid−vapor-like interface. In particular, in the large length scale regime, solvent density is depleted at the surface of the solute (the surface is said to be "dry") and the value of the solvation free energy per unit area is close to that of the liquid−vapor surface tension. It is an enthalpic or energetic effect nucleated by the loss of hydrogen bonding in the vicinity of the solute surface. In contrast, at smaller length scales, it is the configuration space available for hydrogen bonding and not the bonding itself that is reduced. This reduction in configuration space is manifested in an unfavorable entropy of solvation that scales with the size of that reduced space, and thus with the solute volume.[6]

These two regimes have very different temperature dependences. At large length scales, where an interface and surface tension are dominant, the solvation free energy decreases with temperature. At small length scales, where entropy is dominant, the low-temperature free energy increases with temperature. This juxtaposition provides experimental evidence that the solvation of small hydrophobic species, such as linear alkanes, is a phenomenon different from that which drives large length scale hydrophobicity−water-vapor equilibrium and the phase separation of oil and water. Kauzmann commented on this fact long ago,[8] and recently, we have suggested that the juxtaposition is significant to the temperature dependence of protein folding.[9] Of course, an assortment of interactions, and not only hydrophobic effects, would appear to be important in protein folding, and this fact brings into question any conclusions based upon the hard sphere model alone. The current paper takes a small step in beginning to address this question by considering the effects of adding attractions between water and hard sphere solutes. Forms and strengths of the attractions we consider are those typical of water−alkane interactions. In the limit of a very large sphere, where the solute surface is effectively planar, our calculations provide an understanding of the differences between water−vapor and water−oil interfaces.

For the case of small hydrophobic species, the effects of water−solute attractions have been examined by Pratt and Chandler.[10] That work argued that since these attractive forces are very small in comparison with hydrogen bond forces, their effects on solvation free energies can be estimated by assuming the water structure around a hard sphere is unaltered by adding an attraction to the water. This physical idea is the essence of first-order perturbation theory (i.e., mean field theory), and it leads to the corresponding simple expressions for the attractive interaction contribution to the free energy.[11,12] In particular, attractive interactions should produce a simple additive contribution to the solvation enthalpy, but no significant effect to the solvation entropy. This approach has proved satisfactory in explaining the solvation and transfer free energies for alkanes,[10] and it is supported by the results of detailed simulation studies.[13,14]

For the case of large hydrophobic species, we show that the physical picture is much the same. However, there is an

* To whom correspondence should be addressed. E-mail: chandler@cchem.berkeley.edu.

10.1021/jp013289v CCC: $22.00
Published on Web 02/02/2002

interesting distinction. Extended hydrophobic surfaces induce the formation of an interface, and translation of the interface occurs with very little free energy cost. At phase coexistence, there is no cost to translate a planar interface; its translational mode is "infinitely soft". At standard conditions, water is not precisely at liquid−vapor phase coexistence, but it is extremely close. As such, a weak attraction can easily move the interface induced by a hydrophobic surface. This movement need not alter hydrogen bonding or the interfacial structure. It simply translates the location of the interface. We illustrate this effect in section III, where we show the effects of increasing the strength of the attraction, eventually reaching that of a water−alkane interface. At that point, the interface has been drawn into contact with the hydrophobic surface, giving an average interfacial density profile that is very similar to that found with simulations of water between "paraffin" walls.[15−17] While drawn into contact, it is still very much the drying interface that characterizes the density of water near an extended hard wall without attractions. Thus, we show in section III that the crossover for solvating hard spheres is also present for solvating hard spheres that attract water. The absolute values of free energies differ in the two cases, but the differences are primarily those of a simple energetic contribution. Indeed, we show in section IV that the temperature dependence for solvating hard spheres, both small and large, is essentially unaffected by adding water−solute attractions.

The ability of weak attractions to translate the drying interface can be gleaned from the results of an ingenious simulation study by Wallqvist et al.[18] They examined a sphere of water embedded in a continuum of an alkane-like material, treating cavities of up to 24 Å in radius. Although providing some thermodynamic information, their work did not yield solvation free energies. Other studies of hydrophobic solvation in the presence of solute−solvent attractions have been confined to relatively small solutes.[13,19−26] Until now, therefore, in the presence of solute−solvent attractions, the small and large length scaling of hydrophobic solvation free energies has been unknown.

Before focusing on this scaling in sections III and IV, we begin in the next section with the theory from which our results are derived. This theory is based upon the approach of Lum, Chandler, and Weeks (LCW).[2] That work provides a theory for treating hydrophobicity at small and large length scales. In ref 2, the theory was implemented with a simple parameterization of the equation of state for water. In Sec. II, we improve upon that parameterization to ensure that its prediction of the liquid−vapor density profile is consistent with results of simulation. In addition, in section II, we present formulas that generalize the LCW theory so that it may now be applied to solutes that interact with water with relatively long-ranged attractions as well as with short-ranged repulsions. We turn to this development now.

II. LCW Theory of Solute−Solvent Attractions

Implementation of the LCW theory requires prior knowledge of the equation of state, the liquid−vapor surface tension, and the radial distribution function of the pure solvent, in this case water. The methods used in the LCW theory calculations are described in ref 2 (specifically by eqs 2 through 15).

It is generally possible to partition a typical solute−solvent interaction potential, $\Phi(\mathbf{r})$, into a short-ranged repulsive part, $\Phi_0(\mathbf{r})$, and a longer-ranged and often slowly varying attractive part, $\Phi_1(\mathbf{r})$, as suggested by Weeks, Chandler, and Andersen (WCA).[12] For a spherically symmetric potential,

$$\begin{aligned}\Phi_0(r) &= \Phi(r) - \Phi(r_0), \quad r \le r_0\\ &= 0, \quad r > r_0\\ \Phi_1(r) &= \Phi(r_0), \quad r \le r_0\\ &= \Phi(r), \quad r > r_0\end{aligned} \tag{1}$$

where r_0 is the position of the minimum of $\Phi(\mathbf{r})$.

Strong attractions, coinciding with hydrophilic interactions, are treated in the LCW theory by imposing constraints, as illustrated in ref 2. On the other hand, the addition of a slowly varying attractive potential, $\Phi_1(\mathbf{r})$, results in modification to one of the principal equations of the LCW theory for the slowly varying component of the solvent density, $n(\mathbf{r})$ (eq 5 of ref 2). This equation is changed by adding $\Phi_1(\mathbf{r})$, giving

$$w'(n(\mathbf{r})) - m\nabla^2 n(\mathbf{r}) - 2a'\overline{\langle\delta\rho(\mathbf{r})\rangle} + \Phi_1(\mathbf{r}) = 0 \tag{2}$$

where a' and m are related to the parameters in the van der Waals theory[27] describing the energy density and range of interactions respectively, $w(\rho)$ is the local grand free energy density of a uniform fluid at a density ρ, and $\overline{\langle\delta\rho(\mathbf{r})\rangle}$ is a coarse-graining of the difference between the full equilibrium density, $\langle\rho(\mathbf{r})\rangle$, and $n(\mathbf{r})$. In comparing eq 5 of ref 2 with eq 2, note that $n(\mathbf{r})$ here is the quantity labeled $n_s(\mathbf{r})$ in ref 2.

Small length scale variations in $\langle\rho(\mathbf{r})\rangle$ induced by the short-ranged repulsion, $\Phi_0(\mathbf{r})$, that are not captured by eq 2, are treated in a second step. $\Phi_0(\mathbf{r})$ is first approximated by a hard sphere potential, with an effective hard sphere radius, R, chosen according to the WCA theory[12] to minimize the structural and thermodynamic changes resulting from this approximation. In particular, assuming that $\exp[-\beta\Phi_0(r)]$ is a more rapidly varying function of r than the solute−solvent cavity distribution function, $y(r)$,

$$R \approx \int_0^\infty \mathrm{d}r\{1 - \exp[-\beta\Phi_0(\mathbf{r})]\} \tag{3}$$

where $\beta = (k_B T)^{-1}$. The term $\langle\rho(\mathbf{r})\rangle$ can then be obtained in a manner identical to previous LCW calculations[2] for hard sphere solutes: by assuming the fluctuations of $\rho(\mathbf{r})$ around $n(\mathbf{r})$ obey Gaussian statistics and imposing the constraint that $\langle\rho(\mathbf{r})\rangle = 0$ inside the hard sphere volume, v.[28,29] This gives

$$\begin{aligned}\langle\rho(\boldsymbol{r})\rangle &= n(\mathbf{r}) + \int \mathrm{d}\mathbf{r}'\, c(\mathbf{r}')\chi(\mathbf{r},\mathbf{r}')\\ c(\mathbf{r}) &= 0, \quad \boldsymbol{r} \notin v\end{aligned} \tag{4}$$

Here, $c(\mathbf{r})$ is the solute−solvent direct correlation function, which is expanded in a basis set inside the solute volume, v, with coefficients chosen such that $\langle\rho(\boldsymbol{r})\rangle = 0$ inside the volume.[30] The quantity $\chi(\mathbf{r},\mathbf{r}')$ is the interpolated density−density correlation function, $n(\mathbf{r})\delta(\mathbf{r} - \mathbf{r}') + n(\mathbf{r})n(\mathbf{r}')h(|\mathbf{r} - \mathbf{r}'|)$, where $h(r)$ is the bulk liquid water pair correlation function. (See eq 15 of ref 2.) Equation 4 is identical to eq 6 of ref 2. The term $\Phi_1(\mathbf{r})$ appears only implicity, through the dependence of $n(\mathbf{r})$ on this slowly varying potential in eq 2. The molecular scale van der Waals (MVDW) theory of Weeks and co-workers,[31−33] which is similar to the LCW theory in its treatment of slowly and quickly varying components of the density, uses an analogous approach for determining the response of the fluid to excluded volume constraints.

The free energy of solvation, when attractions are present, is obtained by thermodynamic integration. Applying eqs 2 and 4 in the presence of a potential $\xi\Phi_1(\mathbf{r})$ for $0 \le \xi \le 1$ (i.e., as the

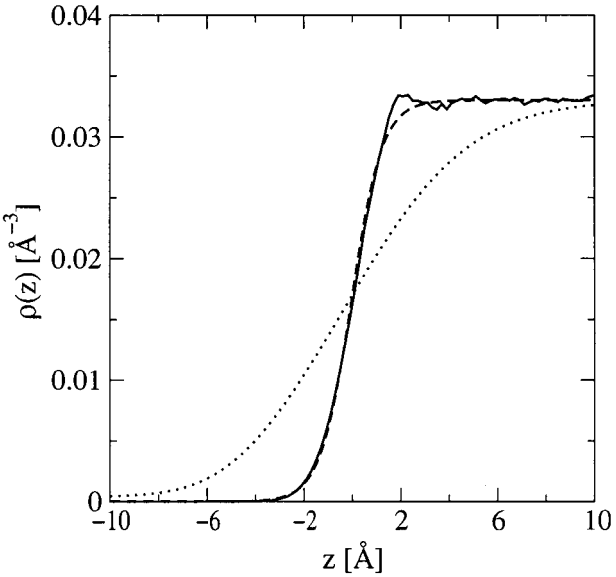

Figure 1. Free liquid−vapor interface profiles at 298 K from a 2 ns molecular dynamics simulation of the SPC/E water model (solid line) (ref 3), using $w(\rho)$ from the original LCW theory of ref 2 (dotted line) and from the parameterization of $w(\rho)$ ($w_{coex}(\rho)$) used in the LCW theory in the present work (dashed line).

attractions are progressively turned on) to obtain $\langle\rho(\mathbf{r})\rangle_\xi$, the solvation free energy when $\Phi_1(\mathbf{r})$ is present is

$$\Delta\mu(\Phi_1) = \Delta\mu(\Phi_1 = 0) + \int_0^1 d\xi \int d\mathbf{r}\Phi_1(\mathbf{r})\langle\rho(\mathbf{r})\rangle_\xi \equiv \Delta\mu_0 + \Delta\mu_{att} \quad (5)$$

The free energy without attractions, $\Delta\mu_0 \equiv \Delta\mu(\Phi_1 = 0)$, is determined using eqs 8 and 9 of ref 2.

One of the goals of the present work is the prediction of the solvent structure outside solutes when solute−solvent attractions are present. It is therefore important that the solvent density in the absence of attractions is described correctly. The simple van der Waals form of the free energy density $w(\rho)$ used for water in the original LCW work (eq 12 of ref 2), however, predicts a free liquid−vapor interface that is significantly broader than that obtained in computer simulations of the SPC/E water model at 298 K, as shown in Figure 1. The liquid−vapor surface tension[3] of the SPC/E model[34] agrees with experiment[35] at 298 K, and may therefore be expected to capture the interfacial behavior of water at this temperature.

We have instead chosen a $w(\rho)$ that correctly describes the free liquid−vapor interface of the SPC/E water model at coexistence at 298 K. In the square gradient theory for a free planar liquid−vapor interface (eq 2 with only the first two terms),[27] it can be shown that for a density profile of the form

$$n(z) = \langle\rho(z)\rangle = \frac{1}{2}\left[(\rho_l + \rho_g) + (\rho_l - \rho_g)\tanh\left(\frac{z}{d}\right)\right] \quad (6)$$

the free energy density is

$$w_{coex}(\rho) = \frac{2m}{d^2(\rho_l - \rho_g)^2}(\rho - \rho_l)^2(\rho - \rho_g)^2 \quad (7)$$

Here, ρ_l and ρ_g are the liquid and vapor densities respectively and d is a parameter that describes the width of the interface. In the square gradient theory, m is also related to $w_{coex}(\rho)$ and the liquid−vapor surface tension, γ (eq 13 in ref 2). For $w_{coex}(\rho)$ in eq 7, $m = 3d\gamma/(\rho_l - \rho_g)^2$.[36] To approximate the proximity to coexistence of water at ambient conditions (temperature, T, of 298 K and pressure, p, of 1 atm) in our calculations with solutes, we have added to $w_{coex}(\rho)$ in eq 7 a term linear in ρ such that $w(\rho_g) - w(\rho_l) \approx p = 1.0$ atm, i.e.,

$$w(\rho) = w_{coex}(\rho) + \frac{\rho - \rho_l}{\rho_g - \rho_l}p \quad (8)$$

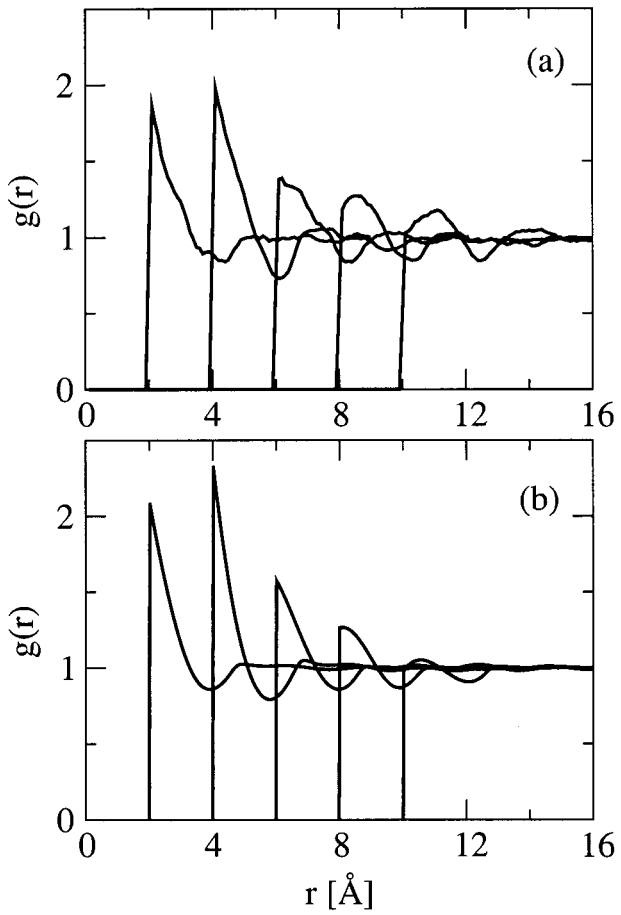

Figure 2. Radial distribution function, $g(r)$, as a function of distance, r, from the solute center for hard sphere solutes with radii $R = 2.0$, 4.0, 6.0, 8.0, and 10.0 Å in SPC/E water at 298 K and 1.0 atm from (a) Monte Carlo (MC) simulations and (b) from the parameterization of LCW theory in this work. The simulations were constant NPT MC simulations of 256, 500, 864, 1372, and 2048 particles respectively for $R = 2.0$, 4.0, 6.0, 8.0, and 10.0 Å and were 200 000 cycles in length for $R = 2.0$, 4.0, and 6.0 Å and 100 000 cycles for $R = 8.0$, and 10.0 Å.

For a simple nonpolar fluid, the parameter a' in eq 2 will be equal to a, where $-a\rho_l^2$ is the attractive energy density of the uniform liquid. Orientational degrees of freedom in a polar fluid such as water make things more complex. We have chosen to modify the unbalanced force parameters so that solvent density profiles calculated using the LCW theory agree with simulations of SPC/E water outside solutes with radii, R, up to 10 Å, as shown in Figure 2. Hence, we take $a' = 350.0$ kJcm^3/mol^2 and coarse-grain the density over a length scale of $\lambda = 3.0$ Å. Although the choice of a' and λ can significantly affect the solvent density profiles outside small solutes, we find that the solvent density outside large solutes is largely insensitive to variations in these quantities. Our results in the $R \rightarrow \infty$ limit are therefore independent of this choice. Furthermore, even for the small solutes shown in Figure 2, simultaneously increasing

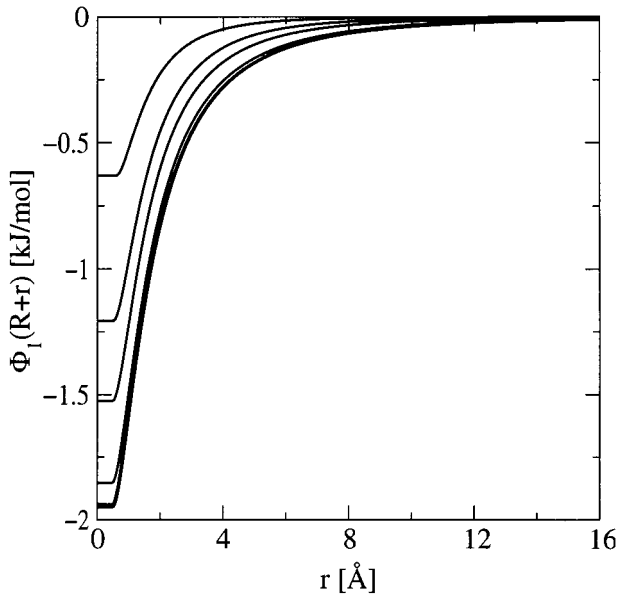

Figure 3. Attractive part of solute−solvent potential, $\Phi_1(r)$, for solutes with effective hard sphere radii $R = 4$, 10, 20, 100, 1000, and ∞ Å (depth of potential well increases with solute size). The curves for $R = 1000$ Å and $R \rightarrow \infty$ are essentially indistinguishable.

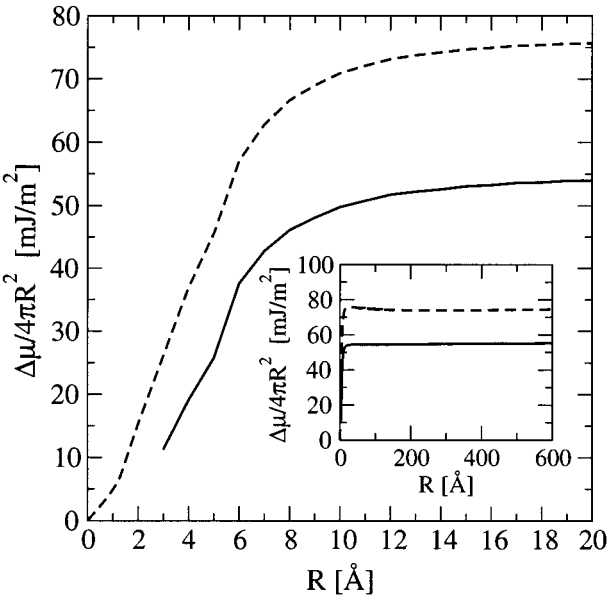

Figure 4. Excess chemical potential per solute surface area, $\Delta\mu/4\pi R^2$, for spherical solutes of radius R in water at 298 K, with (solid line) and without (dashed line) attractive interactions with the solvent. The inset shows the same curves, but for a larger range of R. The solid line does not extend to $R = 0$ because R_s becomes negative for $R \approx 0.6\sigma$.

or decreasing both a' and λ by up to 30% from the values we have used changes the contact densities, $g(R^+)$, by less than 15%.

III. Application to a Water−Alkane Interface

To estimate $\Phi(r)$ for a spherical collection of alkane molecules in water, we assume a uniform density, ρ, of CH_3/CH_2 groups interacting with water via the Lennard-Jones (LJ) potential

$$u_{LJ}(r) = 4\epsilon\left[\left(\frac{\sigma}{r}\right)^{12} - \left(\frac{\sigma}{r}\right)^{6}\right] \tag{9}$$

Integrating $u_{LJ}(r)$ over the volume of a solute of radius R_s, the full attractive interaction with a solvent molecule at distance r from the center of the solute is

$$\Phi(r) = \pi\epsilon\rho\sigma^3\left[\frac{4}{5}\sigma^9\left(\frac{1}{8rr_+^8} - \frac{1}{9r_+^9} - \frac{1}{8rr_-^8} + \frac{1}{9r_-^9}\right) - 2\sigma^3\left(\frac{1}{2rr_+^2} - \frac{1}{3r_+^3} - \frac{1}{2rr_-^2} + \frac{1}{3r_-^3}\right)\right] \tag{10}$$

with $r_+ = r + R_s$ and $r_- = r - R_s$. The hard sphere radius of the solute, R, is related to R_s according to eq 3.

For the alkane−alkane LJ parameters and density, we have used the same values as those employed by Lee et al.[15,16] and Shelley and Patey,[17] chosen to mimic the interaction of water with a material like paraffin (where the LJ parameters are $\sigma_{AA} = 3.768$ Å and $\epsilon_{AA} = 1.197$ kJ/mol, and $\rho = 0.0240$ Å^{-3} (see ref 15). These parameters are also very similar to those employed by Wallqvist et al. for a water droplet embedded in an alkane material.[18] The LJ parameters for the alkane−water interactions in eq 10 were determined using the Lorentz−Berthelot combining rules, with $\sigma = \sigma_{AW} = (\sigma_{AA} + \sigma_{WW})/2 = 3.468$ Å and $\epsilon = \epsilon_{AW} = \sqrt{\epsilon_{AA}\epsilon_{WW}} = 0.882$ kJ/mol, where $\sigma_{WW} = 3.167$ Å and $\epsilon_{WW} = 0.650$ kJ/mol are the water−water LJ parameters in the SPC/E model.[34] $\Phi_1(r)$ is plotted in Figure 3 for several different solute radii R. Hereafter, for convenience we will refer to solutes for which $\Phi_1(r)$ is nonzero outside the solute as "alkane solutes", and as "hard spheres" otherwise.

The excess solvation free energy per solute surface area, $\Delta\mu/4\pi R^2$, from the LCW theory for alkane solutes and hard spheres at 298 K is plotted in Figure 4. The scaling of $\Delta\mu$ with R is qualitatively very similar in both cases. For small solutes, $\Delta\mu$ scales with solute volume, crossing over to an approximate scaling with surface area at around 1 nm.

To obtain the surface tension of the solute−solvent interface, $\tilde{\gamma}$, in the limit $R \rightarrow \infty$, we assume that

$$\frac{\Delta\mu}{4\pi R^2} \approx \frac{pR}{3} + \tilde{\gamma}\left(1 - \frac{2\delta}{R}\right) \tag{11}$$

as discussed in detail in ref 3. Here, $p \approx w(\rho_g) - w(\rho_l)$[38] is the external pressure of 1 atm and δ is a coefficient which describes the approach of an asymptotic scaling of $\Delta\mu$ with surface area. From a linear regression of $\Delta\mu/4\pi R^2$ for R between 200 and 600 Å, we find that $\tilde{\gamma}$ is 53.2 and 72.1 mJ/ m^2, respectively, for the alkane and hard sphere surfaces. The latter value is by construction equal to the liquid−vapor surface tension, γ, one of the input parameters in the theory. The former value is not predetermined and is found to be close to the experimentally measured alkane−water surface tensions at 293 K, which, for all linear alkanes with 6 to 14 carbons, lie between 50.2 and 52.2 mJ/m^2.[39] There do not appear to be experimental measurements at 298 K. However, the values at 298 K are not expected to be significantly different, considering the small change in experimental liquid−vapor surface tensions (around 1 mJ/m^2) for water and alkanes over this temperature range.[37] Our results are also in agreement with the experimentally measured factor of 3 difference between the typical alkane−water surface tension (≈50 mJ/m^2) and the free energy of solvation per surface area of small linear alkanes in water (≈17 mJ/m^2 for $R \approx 4.0$ Å).[6,7] While this difference has been the focus of some interest,[40−44] the difference is essentially a trivial consequence of the crossover behavior illustrated in Figure 4.

The solvent radial distribution function around alkane and hard sphere solutes, $g(R + r)$, is plotted for several radii in

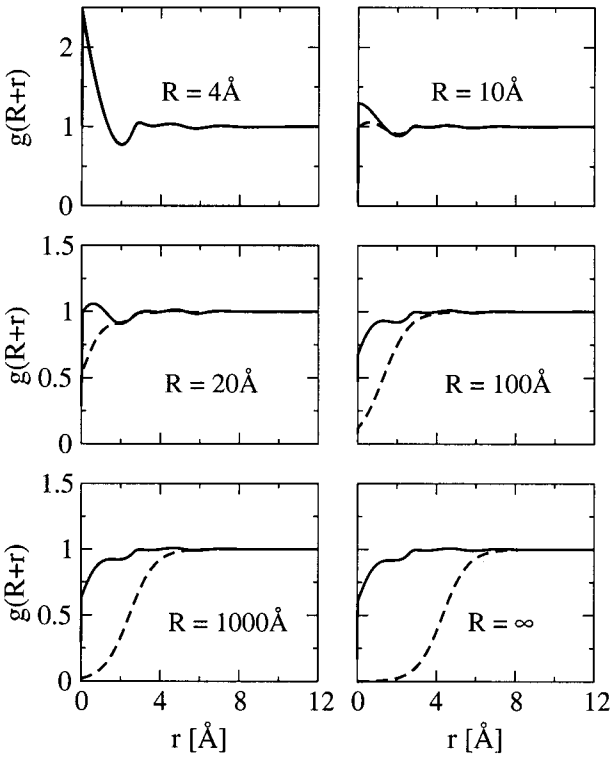

Figure 5. Radial distribution functions, $g(r)$, for water density outside spherical solutes of various radii R at 298 K calculated with (solid lines) and without (dashed lines) solute−solvent attractions.

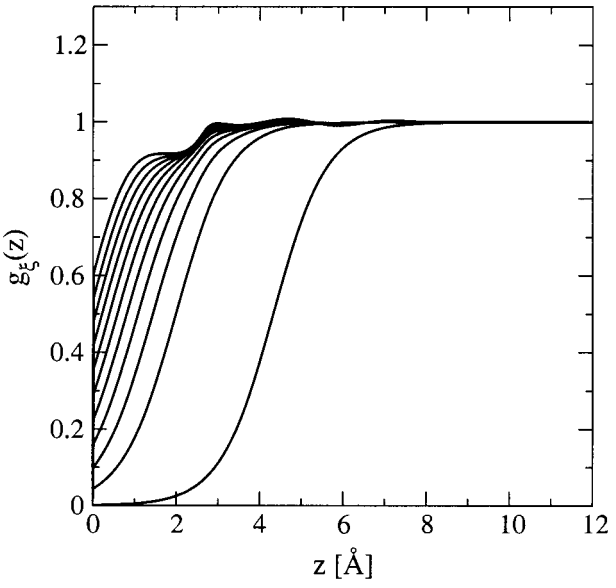

Figure 6. Solvent distribution functions, $g_\xi(z)$, for water outside a wall in the presence of a potential $\xi\Phi_1(r)$, for $\Phi(r)$ in eq 10 and $\Phi_1(r)$ given by eq 1, and ξ at intervals of 0.1 between 0 and 1.0.

Figure 5. For small solutes, there is little difference between the solvent structure when attractions are present or absent, as previously appreciated theoretically[10] and as observed in simulations.[14] However, for large solutes, attractions do have a notable effect, translating the drying interface, as illustrated with varying strengths of attraction in Figure 6. There is little free energy cost to move the liquid−vapor interface because the fluid is close to liquid−vapor phase coexistence. Due to this ease of translation, the addition of an attractive potential as weak as that between alkanes and water is sufficient to draw the drying interface into contact with the hydrophobic surface. For all $R \geq 100$ Å, $g(r)$ for the peak in the first solvation shell is around 0.9. This result is similar to that of Wallqvist et al.[18] for a spherical droplet of radius 21 Å of SPC/E water at equilibrium in an alkane material at 298 K and 1 atm. In those calculations, the corresponding value for $g(r)$ was approximately 1.0, using an attractive interaction potential about 20% stronger than that employed in this work. Our result is also consistent with the computer simulations of Lee et al.[15,16] and of Shelley and Patey,[17] in which it was found that $g(r) \approx 1.12$ for the first solvation shell peak for TIP4P water between parallel alkane plates. One would expect the TIP4P $g(r)$ at contact to be slightly larger than we predict for real water or SPC/E water because the liquid−vapor surface tension of TIP4P water at 300 K, at 63.5 ± 5 mJ/m^2,[45] is smaller than that of either of these two fluids. TIP4P water may therefore be expected to have a "softer" interface, which is thus more easily deformed than that of real water.

While drawn into contact with the large hydrophobic surface, this interface is distinct from the interface that surrounds a small hydrophobic surface. Small solutes have wetting interfaces and solvation free energies that scale with solute volume, while large solutes have drying interfaces, with or without attractions, and solvation free energies that scale with solute surface area. Furthermore, the contact values of $g(R + r)$ for the large hydrophobic solutes are close to 1 or smaller while the small hydrophobic solute considered in Figure 5 has a contact value larger than 2. To within a few tenths, the effect of water−solute attractions on $g(R + r)$ for a large solute is that of simply translating the value of r for $g(R + r)$. Differences of a few tenths are physically unimportant. They coincide with free energy differences that are a small fraction of k_BT.

IV. Temperature Dependence of Hydrophobic Solvation

We have previously studied the temperature and length scale dependence of hard sphere solvation.[9] There, it was suggested that hard sphere solvation should provide an adequate description of the temperature dependence for more complex solutes, such as amino acids and proteins, since solute−solvent attractions mainly add energetic but not entropic contributions to the free energy. Here, we consider this suggestion in more detail. The link between the effects of solvent−solute attractions on structure and free energy temperature dependence is understood with the aid of eq 5. For small hydrophobic solutes, the temperature dependence is well understood.[10,14,19] This understanding follows from the facts that $g(r)$ for the solvent outside such solutes is only weakly dependent upon attractions (see Figure 5), that $g(r)$ is only slightly dependent on temperature,[10,46] and that integrals over $g(r)$ for small hard spheres and corresponding alkane solutes are almost identical.[10] As such, applying eq 5, the attractive interaction contribution to the small hydrophobic solute chemical potential, $\Delta\mu_{att}^{(small)}(R, T)$, can be approximated as

$$\begin{aligned}\Delta\mu_{att}^{(small)}(R, T) &= \rho_l(T)\int_0^1 d\xi \int d\mathbf{r}\, \Phi_1(\mathbf{r}; R)\, g_\xi(\mathbf{r}; R, T) \\ &\approx \rho_l(T) \int d\mathbf{r}\, \Phi_1(\mathbf{r}; R)\, g_0(\mathbf{r}; R, 298\ \mathrm{K}) \\ &\equiv \rho_l(T)\, C^{(small)}(R) \qquad (12)\end{aligned}$$

In contrast, the solvent density outside a large solute translates dramatically in response to even a very small solute−solvent attractive potential. At least at 298 K, once the solvent wets the solute surface, increasing the strength of $\Phi_1(r)$ does not significantly change $\langle\rho(r)\rangle$, as shown in Figure 6. This behavior

can be approximated as

$$\langle \rho(r) \rangle_{\xi} \approx \langle \rho(r) \rangle_0 + \theta(\xi)[\langle \rho(r) \rangle_1 - \langle \rho(r) \rangle_0] \qquad (13)$$

where $\theta(\xi) = 1$ for $\xi \geq 0$ and zero otherwise. Furthermore, assuming that $\langle \rho(r) \rangle_1 \approx \rho_l(T)\theta(r - R)$, which appears to be roughly correct at 298 K, the attractive contribution to the large hydrophobic solute chemical potential, $\Delta\mu_{att}^{(large)}(R, T)$, for large solutes is approximately

$$\Delta\mu_{att}^{(large)}(R, T) \approx \rho_l(T) \int d\mathbf{r}\, \Phi_1(\mathbf{r})\, \theta(r - R) \equiv \rho_l(T) C^{(large)}(R) \qquad (14)$$

At 298 K, eq 14 gives an estimate of $\Delta\mu_{att}^{(large)}(R, T)$ about 40% larger than the value from thermodynamic integration (eq 5 without approximation). Although this discrepancy is significant, we expect the accuracy of the assumptions leading to eq 14 to improve for attractions stronger than the water−alkane interactions treated here. We have also tested the accuracy of eq 14 by carrying out the LCW calculations with $w(\rho)$ parameterized by the simulated SPC/E liquid−vapor density profile and an interpolation of the experimental liquid−vapor surface tension[35] at 367 K.[47] While significantly different profiles are obtained for the free liquid−vapor interface at 298 and 367 K, $g(r)$ near an alkane wall is quite similar. Consequently, the temperature dependence of $\Delta\mu_{att}^{(large)}(R, T)$, as eq 14 would suggest, is almost entirely due to $\rho_l(T)$, with $\Delta\mu_{att}^{(large)}(R, T)/\rho_l(T)$ differing by only 17% at the two temperatures. Therefore, although our assumptions do not capture the full temperature dependence, we expect them to be reasonably accurate. For the alkane−water attractions used in our calculations, eq 14 also appears to provide an upper bound to the magnitude of $\Delta\mu_{att}^{(large)}(R, T)$.

Equations 12 and 14 show that the functional form of the temperature dependence is the same for small and large solutes, but with different temperature-independent prefactors. Per solute surface area, the effect of attractions on the temperature dependence is slightly greater in absolute terms for larger solutes, mainly due to the larger $\Phi_1(r)$ [$C^{(large)}(R)/4\pi R^2 \approx -4.9$ kJÅ/mol for $R \rightarrow \infty$ while $C^{(small)}(R)/4\pi R^2 \approx -2.5$ kJÅ/mol for $R = 3.3$ Å].

Using eqs 12 and 14 and experimentally measured coexisting densities for water,[48] we have calculated the free energy of solvation as a function of temperature for a small methane-sized solute and a planar alkane surface in water and plot the results in Figure 7. For both the small and large solutes, the temperature dependence of $\Delta\mu$ changes only slightly with the addition of attractions. This is shown by the difference between the solid and dotted lines in Figure 7, which differ according to how $\Delta\mu_{att}^{(large)}(R, T)$ and $\Delta\mu_{att}^{(small)}(R, T)$ at a general temperature, T, differ from their respective quantities at $T = 298$ K. For the small solute, the maximum in $\Delta\mu$, where the molar entropy of solvation $\Delta s = -(\partial\Delta\mu/\partial T)_p = 0$, shifts from a temperature of 386 K to 396 K. The temperature shift is similar to that observed in simulations.[14] This shift is a small effect, considering that changing the radius of a hard sphere solute from 3.3 to 4.0 Å shifts the maximum by more than 35 K.[9]

The relatively small effect of attractions and the similar trends found for both small and large solutes indicate that our previous findings on hydrophobic solvation, and entropies of protein unfolding in particular, which were based on hard sphere solvation,[9] remain virtually unchanged.

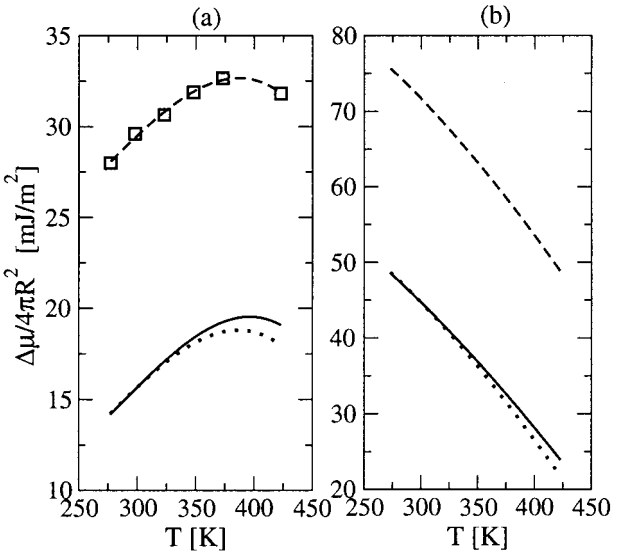

Figure 7. Excess chemical potential per solute surface area, $\Delta\mu(R, T)/4\pi R^2$, as a function of temperature with (solid line) and without (dashed line) attractions for (a) a solute of radius $R = 3.3$ Å and (b) a planar surface. The dotted lines are $\Delta\mu_0(R, T) + \Delta\mu_{att}(R, T = 298\ K)$. For the planar surface, the dashed line, $\Delta\mu_0/4\pi R^2$, is taken as the experimental liquid−vapor surface tension (ref 35).

Acknowledgment. This work was supported by the Director, Office of Science, Office of Basic Energy Sciences, of the U.S. Department of Energy under Contract No. DE-AC03-76SF00098.

References and Notes

(1) Stillinger, F. H. *J. Solution Chem.* **1973**, *2*, 141.
(2) Lum, K.; Chandler, D.; Weeks, J. D. *J. Phys. Chem. B* **1999**, *103*, 4570.
(3) Huang, D. M.; Geissler, P. L.; Chandler, D. *J. Phys. Chem. B* **2001**, *105*, 6704.
(4) Ten Wolde, P. R.; Sun, S. X.; Chandler, D. *Phys. Rev. E* **2002**, *65*, 011201.
(5) Sun, S. X. *Phys. Rev. E* **2001**, *64*, 021512.
(6) Small linear alkanes ($\lesssim$10 carbons) in water are in the small length scale regime. Their solvation free energies are often viewed as scaling with solute surface area (ref 7). This view does not contradict the fact that in the small length scale regime, free energies properly scale with volume. In the case of small linear alkanes, surface area is approximately proportional to volume.
(7) Tanford, C. *The Hydrophobic Effect − Formation of Micelles and Biological Membranes*; Wiley-Interscience: New York, 1973.
(8) Kauzmann, W. *Adv. Prot. Chem.* **1959**, *14*, 1.
(9) Huang, D. M.; Chandler, D. *Proc. Natl. Acad. Sci., U.S.A.* **2000**, *97*, 8324.
(10) Pratt, L. R.; Chandler, D. *J. Chem. Phys.* **1977**, *67*, 3683.
(11) Chandler, D. *Introduction to Modern Statistical Mechanics*; Oxford University Press: New York, 1987; Chapter 7.
(12) Chandler, D.; Weeks, J. D.; Andersen, H. C. *Science* **1983**, *220*, 787.
(13) Gallicchio, E.; Kubo, M. M.; Levy, R. M. *J. Phys. Chem. B* **2000**, *104*, 6271.
(14) Guillot, B.; Guissani, Y. *J. Chem. Phys.* **1993**, *99*, 8075.
(15) Lee, C. Y.; McCammon, J. A.; Rossky, P. J. *J. Chem. Phys.* **1984**, *80*, 4448.
(16) Lee, S. H.; Rossky, P. J. *Proceedings of the 10th Korean Scientists and Engineers Conference*, Inchen, Korea, 1987; p 150.
(17) Shelley, J. C.; Patey, G. N. *Mol. Phys.* **1996**, *88*, 385.
(18) Wallqvist, A.; Gallicchio, E.; Levy, R. M. *J. Phys. Chem. B* **2001**, *105*, 6745.
(19) Garde, S.; García, A. E.; Pratt, L. R.; Hummer, G. *Biophys. Chem.* **1999**, *78*, 21.
(20) Beutler, T. C.; Béguelin, D. R.; van Gunsteren, W. F. *J. Chem. Phys.* **1995**, *102*, 3787.
(21) Floris, F. M.; Selmi, M.; Tani, A.; Tomasi, J. *J. Chem. Phys.* **1997**, *107*, 6353.
(22) Jorgensen, W. L.; Ravimohan, C. *J. Chem. Phys.* **1985**, *83*, 3050.
(23) Guillot, B.; Guissani, Y.; Bratos, S. *J. Chem. Phys.* **1991**, *95*, 3643.
(24) Hummer, G.; Pratt, L. R.; García, A. E. *J. Phys. Chem.* **1996**, *100*, 1206.

(25) Lynden-Bell, R. M.; Rasaiah, J. C. *J. Chem. Phys.* **1997**, *107*, 1981.
(26) Kalko, S. G.; Sesé, G.; Padró, J. A. *J. Chem. Phys.* **1996**, *104*, 9578.
(27) Rowlinson, J. S.; Widom, B. *Molecular Theory of Capillarity*; Oxford University Press: Oxford, 1982; Chapter 3.
(28) Chandler, D. *Phys. Rev. E* **1993**, *48*, 2898.
(29) It is also assumed that $\delta\rho(\mathbf{r})$ does not couple to $\Phi_1(\mathbf{r})$ in the Hamiltonian for the density.
(30) We find that a single basis function, a constant, is adequate in most cases for describing $\langle\rho(\mathbf{r})\rangle$ outside solutes.
(31) Weeks, J. D. *Annu Rev. Phys. Chem.* **2002**, *53*, 533.
(32) Katsov, K.; Weeks. J. D. *Phys. Rev. Lett.* **2001**, *86*, 440.
(33) Vollmayr-Lee, K.; Katsov, K.; Weeks, J. D. *J. Chem. Phys.* **2001**, *114*, 466.
(34) Berendsen, H. J. C.; Grigera, J. R.; Straatsma, T. P. *J. Phys. Chem.* **1987**, *91*, 6269.
(35) Vargaftik, N. B.; Volkov, B. N.; Voljak, L. D. *J. Phys. Chem. Ref. Data.* **1983**, *12*, 817.
(36) For γ, we have used the experimental surface tension of water of 71.99 mJ/m^2, which is almost identical to the surface tension of the SPC/E model of 73.6 ± 2 mJ/m^2 (ref 3). We have also used the experimental vapor pressure (ref 37) and the ideal gas law to obtain the vapor density, $\rho_g = 7.7 \times 10^{-7}$ Å^{-3}. $\rho_l = 0.03294$ Å^{-3} and $d = 1.27$ Å were obtained by fitting the simulated liquid−vapor interface to eq 6. This gives $m = 919.9$ kJ mol^{-2} cm^3 Å^2.
(37) *CRC Handbook of Chemistry and Physics*, 2nd electronic ed., 80th ed.; CRC Press: Cleveland, 1999/2000.
(38) For the range of solute radii R used in the regression, volume-dependent terms in the free energy proportional to the vapor density, ρ_g, which are discussed in some detail in ref. 3, are not significant.
(39) Fowkes, F. M. *J. Phys. Chem.* **1963**, *67*, 2538.
(40) Tanford, C. *Proc. Natl. Acad. Sci. U.S.A.* **1979**, *76*, 4175.
(41) Sharp, K. A.; Nicholls, A.; Fine, R. F.; Honig, B. *Science* **1991**, *252*, 106.
(42) Ashbaugh, H. S.; Kaler, E. W.; Paulaitis, M. E. *J. Am. Chem. Soc.* **1999**, *121*, 9243.
(43) Sitkoff, D.; Sharp, K. A.; Honig, B. *Biophys. Chem.* **1994**, *51*, 397.
(44) Chan, H. S.; Dill, K. A. *Annu. Rev. Biophys. Biomol. Struct.* **1997**, *26*, 425.
(45) Pohorille, A.; Wilson, M. A. *J. Mol. Struct. (THEOCHEM)* **1993**, *284*, 271.
(46) Bridgeman, C. H.; Buckingham, A. D.; Skipper, N. T. *Chem. Phys. Lett.* **1996**, *253*, 209.
(47) $\gamma = 60.1$ mJ/m^2, $\rho_l = 0.03158$ Å^{-3}, $\rho_g = 1.6 \times 10^{-5}$ Å^{-3}, $d = 1.65$ Å, and $m = 1080$ kJ mol^{-2} cm^3 Å^2.
(48) http://webbook.nist.gov/chemistry/. $\rho_l(T)$ along the coexistence curve was fit to a cubic. For ρ_l in units of Å^{-3} and T in K, $\rho_l(T) \approx 0.016517 + 0.00014517T - 3.7854\times10^{-7}T^2 + 2.7053\times10^{-10}T^3$.